Effect of graphene oxide-carbon nanotube hybrid filler on the mechanical property and thermal response speed of shape memory epoxy composites

Enliang Wang, Yubing Dong, MD Zahidul Islam, Laiming Yu, Fuyao Liu, Shuaijie Chen, Xiaoming Qi, Yaofeng Zhu, Yaqin Fu, Zhaohe Xu, Ning Hu

PII: S0266-3538(18)31729-9

DOI: https://doi.org/10.1016/j.compscitech.2018.11.022

Reference: CSTE 7465

To appear in: *Composites Science and Technology*

Received Date: 18 July 2018

Revised Date: 6 November 2018

Accepted Date: 12 November 2018

Please cite this article as: Wang E, Dong Y, Islam MZ, Yu L, Liu F, Chen S, Qi X, Zhu Y, Fu Y, Xu Z, Hu N, Effect of graphene oxide-carbon nanotube hybrid filler on the mechanical property and thermal response speed of shape memory epoxy composites, *Composites Science and Technology* (2018), doi: https://doi.org/10.1016/j.compscitech.2018.11.022.

Effect of graphene oxide-carbon nanotube hybrid filler on the mechanical property and thermal response speed of shape memory epoxy composites

Enliang Wang[a], Yubing Dong[a]*[1], MD Zahidul Islam[a], Laiming Yu[a], Fuyao Liu[a], Shuaijie Chen[a], Xiaoming Qi[a], Yaofeng Zhu[a], Yaqin Fu[a], Zhaohe Xu[b], Ning Hu[b]*[2]

[a]*Key Laboratory of Advanced Textile Materials and Manufacturing Technology Ministry of Education, Zhejiang Sci-Tech University, Hangzhou, Zhejiang 310018, China*

[b]*College of Aerospace Engineering, and The State Key Laboratory of Mechanical Transmissions, Chongqing University, Chongqing 400044, China*

a*1 Corresponding author: Yubing Dong; E-mail: dyb19831120@zstu.edu.cn.

b*2 Corresponding author: Ning Hu; E-mail: ninghu@cqu.edu.cn.

Effect of graphene oxide-carbon nanotube hybrid filler on the mechanical property and thermal response speed of shape memory epoxy composites

Enliang Wang[a], Yubing Dong[a*1], MD Zahidul Islam[a], Laiming Yu, Fuyao Liu[a], Shuaijie Chen[a], Xiaoming Qi[a], Yaofeng Zhu[a], Yaqin Fu[a], Zhaohe Xu[b], Ning Hu[b*]

[a]*Key Laboratory of Advanced Textile Materials and Manufacturing Technology Ministry of Education, Zhejiang Sci-Tech University, Hangzhou, Zhejiang 310018, China*

[b]*College of Aerospace Engineering, and The State Key Laboratory of Mechanical Transmissions, Chongqing University, Chongqing 400044, China*

Abstract

Shape memory polymers (SMPs) will come to act an indispensable part in numerous aspects of human activity. However, the low mechanical strengths and thermal conductivities of SMPs have largely restricted their applications. Remarkable improvements in the mechanical properties and thermal conductivities of SMPs via introducing thermal conductivity fillers have been achieved, though the fillers acted as obstructors or promoters for the thermal response speed of SMPs were unclear. In the present study, ternary hybrid polymeric shape memory composites of graphene oxide/carbon nanotube/waterborne epoxy (GO/CNT/WEP) were fabricated, where GO acted as a non-covalent dispersant for CNT in WEP and as a reactive secondary reinforcing agent to improve the mechanical strength and thermal conductivity of WEP. The experimental results showed that GO and CNT were uniformly dispersed and well incorporated into WEP matrix, significantly enhanced the mechanical properties, thermal conductivity and thermal response speed of the GO/CNT/WEP composites.

---

*Corresponding author: Yubing Dong; E-mail: dyb19831120@zstu.edu.cn.

*Corresponding author: Ning Hu; E-mail: ninghu@cqu.edu.cn.

Moreover, the thermal response speed of the shape memory composites was controlled by their thermal conductivity at low filler content, while the storage modulus was the dominant factor for the thermal response speeds of the shape memory composites at filler content higher than 2wt%.

Keywords: A. Smart materials; A. Polymers; A. Nano particles; B. Thermomechanical properties

1. Introduction

Shape memory polymers (SMPs) is one of the most essential branches of smart materials, which have attracted a large amount of attention from both academia and industries. SMPs can maintain a temporary shape and subsequently recover their initial shape upon exposure to appropriate external stimuli, such as water, pH, light, heat, electric and magnetic fields [1-5]. SMPs possess many outstanding aspects, such as easy processibility, ultra-high shape memory recover ratio, low cost, lightweight, good biodegradability, and adjustable shape memory transformation temperature. Recently, Li et al. made an exciting discovery and reported that enthalpy lead a higher recovery stress and energy output than that of the traditionally entropy driven shape memory effect, even comparable to shape memory alloys (SMAs) [6]. Today, SMPs can be applied in many areas, including aerospace industry, automobile, intelligence textile, sensor, information carrier, biomedicine, and household products, and so on. However, SMPs have lower mechanical strengths and thermal conductivities than that of SMAs, which have greatly restricted their wide applications in human life [1-4].

Fortunately, mixing a small amount of reinforcing filler can improve can significantly improve the mechanical strengths and thermal conductivities of SMPs physical and chemical cross-linking with each other [7-10]. Carbon nanotubes (CNTs) are the most popular material amongst all the other carbon-based fillers. The CNTs are considered as novel materials that can be used as filler, because of their excellent physical property, chemical stability, availability, small diameter, and low density. The performance of SMPs can be improved such as mechanical strengths, thermal conductivities, and electrical conductivity by reinforcing of the SMPs. However, CNTs tends to agglomerate and entangle because of strong van der Waals forces and a high aspect ratio at a higher content, thereby the biggest challenge is a homogeneous dispersion of the CNTs in SMP matrix [11]. Several methods have been used to efficiently disperse the CNTs such as ultrasonication, in-situ chemical polymerization, covalent and non-covalent functionalization of CNTs [12-16]. The non-covalent functionalization of CNTs with surfactant or polymer is one of the most effective methods. Probably, the surface of CNTs adsorbs various functional groups without disturbing the π-π conjugate between graphene sheets after functionalization of CNT. The resultant sheets may have a lower surface tension which may improve the compatibility between CNT and the polymer matrix [12].

According to recent studies, two-dimensional (2D) graphene oxide (GO) can act as a highly effective dispersion agent for one-dimensional (1D) CNT to form solution-like aqueous suspension in the fabrication of conductive coatings or films. The 2D structure tethered with considerable functional groups possesses GO sheet of the dual molecule-colloid characteristic, which makes it behave like a molecular as well as a colloidal surfactant [16, 17]. GO-treated CNTs overcome the substantial van der Waals forces, intermolecular and internal molecular interaction through electrostatic and steric repulsive forces and effectively prevents the agglomeration of CNT [17]. Moreover, GO is typically obtained by exfoliation of graphite sheets under strong acidic and oxidative conditions. The process introduces oxygen-containing (OH) groups, which can improve the compatibility and interfacial adhesion between GO and the polymer matrix to acquire high-performance composites [18-21].

In our previous research, we found that waterborne epoxy (WEP) with excellent shape memory performance and its mechanical property was significantly enhanced via adding CNT [17, 22]. However, it was difficult to disperse CNT in WEP matrix uniformly, especially at high CNT content. In the present study, GO was introduced to the CNT-WEP system as a non-covalent dispersant for CNTs and a reactive secondary reinforcing agent to prepare high performance GO/CNT/WEP shape memory composites. The synergetic effect of 2D GO and 1D CNT on the mechanical and thermal properties of the shape memory composites were presented and discussed. Moreover, the impact of the CNT as a filler in the resultant hybrid structure for the thermal conductivity and thermal respond speed of the composites was investigated. It is known that the filler can restrain the molecular chain mobility of the polymer matrix, increased the storage modulus and recovery of the shape memory composites. On the other hand, the thermal conductivity of the polymer matrix can be significantly improved by the addition of small amount of thermal conductivity filler, which is constructive for thermal response speed of SMPs. Since CNT and GO are two excellent thermal conductivity carbon material as a filler and dispersing agent, which can be used for mechanical reinforcements, and behave like obstructors or promoters for the thermal response speed of SMPs. To test the hypothesis, the relation among the thermal conductivity, storage modulus, and thermal response speed were systematically studied based on the GO/CNT/WEP shape memory composites.

2. Materials and methods

2.1. Materials

WEP (AB-EP20 emulsion, 50% solid content) and amine based waterborne curing agent (AB-HGF, Zhejiang An bang New Material Development Co., Ltd, China), and ultra-pure water were obtained from commercial sources. GO was prepared in our lab according to a modified Hummer's method [23]. Nature flake graphite (100 mesh, metal basis) and analytical grade $KMnO_4$, CrO_3, 98% H_2SO_4, hydrochloric acid (37wt%), and 30wt% H_2O_2 aqueous solution were purchased from Aldrich. CNTs were obtained from Showa Denko K. K., (Japan) with an average diameter of 80 nm.

2.2. Techniques

2.2.1. Preparation of the composites

The composites were fabricated via an eco-friendly aqueous solution mixing method, and the operating steps were illustrated in **Fig. 1.** CNT powder, GO aqueous solution, and CNT/GO aqueous solution was added into WEP and ultrasonically treated for 30 min, respectively. The curing agent was added into the mixed solution and dispersed to homogeneity by intensive mixing in a beaker at a speed of 10000 r/min for 5 min, and the weight ratio of WEP to the curing agent was 4:1. Then, the above mixture was frozen in liquid nitrogen, and subsequently dried in a Labconco Free Zone freeze-drier operated at 0.1 mbar and -15 °C for two weeks. Finally, the resulting compound powder was compressed into film at 120 °C under a pressure of 10 MPa for 2 h. The final thickness of the films was approximately 0.30-0.50 mm. In this study, CNT and GO share the same proportion in all the GO/CNT/WEP sample with different fraction (1wt%, 2wt%, 4 wt%, and 6 wt%).

2.2.2. Morphology and structure characterization

The dispersion states of CNT and GO in the composites were observed using a field emission scanning electron microscope (SEM, Ultra 55, Zeiss, Germany) and examined under a transmission electron microscope (TEM) operating at 3 kV and 200 kV, respectively. To prepare for TEM imaging, the samples were embedded in in epoxy resin and were ultramicrotomed into thin slices. X-ray diffraction (XRD) spectrum was recorded on a X-ray diffractor (Bruker AXS, Germany) operating at 40 kV with a scan rate of 2 °/min between 5° and 35°.

2.2.3. Thermal conductivity measurement

The thermal conductivities of the composites were conducted based on transient plane source technology using a Hot Disk 2500S instrument (Hot Disk AB, Gothenburg, Sweden). To eliminate the effect of dust and other impurities on the surface of samples， all the samples were cleaned by absolute ethyl alcohol before measurement.

2.2.4. Tensile test and dynamic mechanical analysis (DMA)

The mechanical property tests were performed using a tensile test instrument (Instron Corp, Norwood, Massachusetts, USA) at the speed of 5 mm/min in a constant temperature and humidity test room, and the specimen with a standard dumbbell shape ($500\times4\times0.32$ mm^3). At least five effective specimens were tested for each sample. DMA Q800 (TA, Instruments) was employed in film tension mode for the dynamic mechanical measurements over the range of 20 °C to 100 °C at the heating speed of 3 °C/min. Each sample was cut into the sizes of $30\times10\times0.32$ mm^3 and the thickness was measured before the test.

2.2.5. Thermal mechanical cycle tests

The shape memory properties of the composites were conveniently measured by thermal mechanical cycle tests performed on the TMA Q400 (TA Instruments) in dynamic DMA mode. The samples were pulled with an increasing stress from 0 to 0.75

MPa at 80 °C (>T_g). While keeping the stress at 0.75 MPa, the samples were cooled down to 25 °C (<T_g) and held for 10 minutes. The load was released at 25 °C with a little releasing strain, realizing the shape memory fixity (the loading and unloading speed was 0.5 MPa/min). Then, the samples were heated from 25 °C to 80 °C under no load and held for 10 minutes, resulting in the recovery of the samples' strain. A residual strain would remain when this cycle finished. The heating or cooling speed was 5 °C/min.

3. Results and discussion

3.1. Dispersion of GO and CNT in composites

It is common knowledge that the thermal conductivity and mechanical properties of SMP composites are directly affected by the dispersion condition of filler in the polymer matrix [24]. The morphological composition and structure of the nanocomposites were investigated via SEM. The composites exhibited a rough surface, as shown in **Fig. 2(a)-(f),** implying energy consumption during crack formation and growth. The SEM image of the 4wt% CNT/WEP composite shows several CNT bundles (see **Fig. 2(b) and (e)**). By contrast, a relatively uniform dispersion of CNT in WEP matrix was observed after the addition of GO (see **Fig. 2(c) and (f)**). The filler dispersion was further confirmed by TEM, as shown in **Fig. 2(g)-(i)**. TEM images of the samples containing 4wt% fillers showed that the GO/CNT hybrid filler were homogeneously dispersed in the WEP matrix due to assistant of GO.

Generally speaking, the disappearance of the characteristic XRD diffraction peak for GO sheets in the composites give a demonstration that GO is highly exfoliated into individual GO sheets in the polymer matrix [25, 26]. The XRD spectra of GO, CNT, WEP, and its composites are shown in **Fig. 3(a)**. As expected, a characteristic diffraction peak of GO was observed at 10.3°, corresponding to an interlayer distancing of ~0.86 nm. However, a wide diffraction peak caused by scattering of the cured epoxy molecules appeared from 14° to 26° in the XRD spectra of neat WEP, revealing its intrinsic amorphous quality. It should be pointed out that the GO/WEP composites and the GO/CNT/WEP composites all show similar diffraction pattern as neat WEP. The XRD measurement results obviously demonstrate that GO was highly exfoliated in the WEP composites. The small peak at about 26.5° can be contributed to CNT, as shown in **Fig. 3(a)**. On the other hand, the other possibility is that the peak originated from the presence of a compact stacked planar multilayered carbon structure typical of graphite [27].

3.2. Thermal conductivity of composites

The thermal conductivity coefficients of the composites are shown in **Fig. 3(b).** When the total concentration of the filler (GO, CNT and GO-CNT hybrid) was fixed, a higher thermal conductivity coefficient was observed in the GO/CNT/WEP composites. The thermal conductivity coefficient of the fabricated composites tends to be stable for the GO/WEP composites and the GO/CNT/WEP composites and slightly decrease for the CNT/WEP composites at high filler fraction. Compare to neat WEP, the thermal conductivity coefficients of the GO/WEP and the CNT/WEP composites was improved about to 30-150%. It is important to note that the thermal conductivity coefficients of the GO/CNT/WEP composites were enhanced by 120-350%. Factors contributing to the interesting phenomena may originate from the following two aspects. Firstly, CNT and GO possibly exhibited a synergistic action in enhancing the thermal conductivity coefficient of the composites. Secondly, the addition of GO increased the synergic effect of CNT by reducing the agglomeration, and improved the thermal conductivity coefficient of the composites. The long and tortuous CNT connect neighboring GO sheets, consequently the 1D fibrous CNT and 2D planar GO can form a 3D thermal conductive network structure, resulting in enlarging the contact surface area between hybrid fillers and WEP matrix immensely. The greater contact surface area can provide more available paths for phonon diffusion, and weaken the thermal interfacial resistance [28].

3.3. Mechanical property of composites

Fig. 4(a) and (b) show the mechanical properties of the composites. Obviously, the experimental results indicated that the composites become stiffer than pristine WEP. In addition, the GO/CNT/WEP composites acquire a significant improvement in mechanical strength compared to the composites modified by single GO or CNT. The mechanical strength of the GO/CNT/WEP composites increased 28% and 13% compare to the GO/WEP composites and CNT/WEP composites at the same filler content (1wt%), respectively. The outstanding mechanical strength of the GO/CNT/WEP composites fully demonstrated the synergic reinforcement between GO and CNT on the mechanical properties of the composites. Two factors contributing to the synergic reinforcement effect were proposed: (i) GO make a huge contribution serving as a superior non-covalent surfactant to disperse pristine CNT in water to become more stable suspensions [17]. As shown in **Fig. 4(f)**, GO assisted well insoluble dispersion of CNT in water with ultrasonication and high-speed shear mixing; (ii) it could be highly beneficial for the formation of 1D CNT and 2D GO hierarchically nano-structure and interconnected network architecture which can effectively inhibit the agglomeration of CNT [21]. The good dispersion state enlarged the surface area and better interaction between GO/CNT nanofillers and WEP matrix. In addition, In WEP, there is a small amount of emulsifier for epoxy resin disperses in water. The emulsifier acts as plasticizer in the final film. That is the reason why a yielding point generates in the stress-strain curve. The test result showed that the crosslink density pristine WEP, 1wt% GO/WEP composite, 1wt% CNT/WEP composite and 1wt% GO/CNT/WEP composite was approximately 0.00216, 0.00203, 0.00212, and 0.00208, respectively (tested via equilibrium swelling method). Compared with the pristine WEP, all composites showed slightly lower crosslink density due to fillers impede the crosslinking of the WEP network.

However, the tensile strength of the CNT/WEP composites and the GO/CNT/WEP composites significantly reduced when the nanofillers fraction above 4wt%, as shown in **Fig. 4(b)**. This phenomenon can be attributed to the following two reasons: (i) The GO's promotion cannot further improve the property of CNT tend to form bundle structures due to their substantial van der Waals interaction, especially at high CNT content, which greatly influences the homogenization of composites (see **Fig. 5(c)-(e)**); and (ii) CNT agglomeration would generate steric barrier, blocking WEP flow into CNT bundles, and contributing to the generation of holes and voids between CNT and WEP matrix. Stress concentration originated from these defects lead to poor mechanical property [29]. In addition, the WEP matrix was hard to bond the black filler (CNT, GO, and GO/CNT) together at the high filler fraction. Therefore, the mechanical properties and shape memory performance of the composites were dropped significantly.

3.4. Dynamic mechanical analysis

Regardless of the molecular structure, DMA curves are used to analyzewhether the polymer and its composites have shape memory characteristics [1, 4]. The results of dynamic mechanical measurements are listed in **Table 1,** and the storage modulus and

Tan Delta of the composites at the filler content of 1wt% was plotted as storage modulus (E′) vs temperature (see **Fig. 5(a)**). All composites exhibited similar temperature dependent viscoelasticity characteristics when the temperature was increased from 20 °C to 100 °C. Storage modulus observed two orders of magnitude drop while the composites undergo a thermal revisable glass transition. The storage modulus of the GO/CNT/WEP composites showed an apparent raise before the filler fraction increase to 4wt% (see **Table 1**). Then, it started to decline when the filler fraction above 4wt%. These DMA features indicated that the composites are outstanding SMP composites.

3.5. Shape memory property of composites

Shape memory performance of SMPs can be typically evaluated by the shape fixity ratios (R_f, the capacity to maintain the temporary shape) and shape recovery ratios (R_r, the capacity to recover the initial shape), as defined by Eq. (1) [30, 31]. N represents the number of thermo-mechanical cycles, ε_m represents the strain at the end of fixing, ε_u represents the strain at the end of unloading and ε_p represents the strain at the end of recovery. In the first cycle, the shape recovery ratios of the composites were decreasing after addition of filler. Interestingly, the shape recovery ratios of the composites were more than 99% after the second cycle. The ratios tended to be a constant 100%. This phenomenon is called “training” effect [30], as shown in **Fig5. (b)-(e)**.

The thermal response speed is another important property of SMP. **Fig. 5(f)** shows WEP and the 4wt% GO/CNT/WEP composites required approximately 4 s to achieve shape recovery in 80 °C water, while the composites response more rapidly than WEP, especially in preliminary recovery stage. On the other hand, the recovery stress of the composites will generate and release sooner than that of the pristine WEP under the same condition. Therefore, the time interval (from recovery stress generate to release) can effectively represent the improvement of the nanofiller addition on the thermal response speed of the shape memory polymer composites. Furthermore, epoxy system was exactly similar to the crosslinked rubber elastic material, which has vigorous random molecular motion and the recovery stress and the elastic modulus increase with temperature. In other words, under the same isostrain condition at high temperature, the sample has higher recovery stress. Therefore, the temperature fluctuation sensitivity of the recovery stress under isostrain is a method to study the effect of filler addition and composite structure on the thermal response speed of the shape memory polymer composites. The thermal response speeds of the composites were conducted via TMA under the isostrain condition (ε=7.2%) from 40 °C to 80 °C with a same heating and cooling speed 5 °C/min, as shown in **Fig. 6**. Here, the time from the recovery stress formation to release was set as ***t***, as shown in **Fig. 6(a).** For example, if ***t*** value is big, means the thermal response speed is slowly. On the contrary, if ***t*** value is small, means the thermal response speed is fast. Therefore, "**1/*t***" was applied to deformation the thermal response speed of the composites.

The filler significantly improved the thermal response speed of the neat WEP, as shown in **Fig. 6** and **Table 1**. Meanwhile, the synergetic effect of the hybrid filler was also very eye-catching. However, the decreased thermal response speed of the composites over 2wt% can be observed for the GO/CNT/WEP composites, as shown in **Fig. 7**. When the filler content below 2wt%, the promoting effect of thermal conductivity on the thermal response speed was stronger than the inhibitory effect of storage moduli of the composites, which was the dominant factor. Over 2wt%, the inhibitory effect of storage modulus of the composites' was the dominant factor. For the increasing of thermal response speed of the sample 6wt% GO/CNT/WEP composites, might be contributed to the filler aggregation at high filler content result in a low storage modulus.

4. Conclusions

In the present study, solution-like aqueous GO-CNT suspension and the GO/CNT/WEP shape memory composites were successfully fabricated with the assistance of GO, which provides an environment-friendly path to produce good dispersion GO/CNT/WEP composites. The effect of filler addition and composite structure on the mechanical properties and thermal response speeds of the shape memory composites was investigated and discussed.

(1) A remarkable synergetic effect between GO and CNT in improving tensile strength, thermal conductivity, and thermal response speed of the composites was observed and confirmed. The synergetic effect originated from the CNT uniform dispersion, and GO's reinforcement, and 3D network structure formation by 1D CNT and 2D GO.

(2) The hybrid fillers improved the composites' thermal response speed. At low filler content, the thermal conductivity of the composites was the dominant factor for the thermal response speed. While the filler content over 2wt%, the storage modulus of the composites was the dominant factor for the thermal response speed.

Acknowledgements

This work was supported by the National Natural Science Foundation of China (NSFC, Grant No. 51703204 and 51473147), and Key Program for International Science and Technology Cooperation Projects of Ministry of Science and Technology of China (Grant No. 2016YFE0125900).

Appendix

$$R_f(N) = \frac{\varepsilon_{\mathrm{u}}(N)}{\varepsilon_{\mathrm{m}}}, \quad and \quad R_r(N) = \frac{\varepsilon_{\mathrm{m}} - \varepsilon_{\mathrm{p}}(N)}{\varepsilon_{\mathrm{m}} - \varepsilon_{\mathrm{p}}(N-1)} \qquad \text{Eq.(1)}$$

References

[1] Q. Zhao, H. J. Qi, T. Xie, Recent progress in shape memory polymer: New behavior, enabling materials, and mechanistic understanding, Prog. Polym. Sci. 49 (2015) 79-120.

[2] H. Meng, G. Li, A review of stimuli-responsive shape memory polymer composites, Polymer 54 (9) (2013) 2199-2221.

[3] W. Wang, Y. Liu, J. Leng, Recent developments in shape memory polymer nanocomposites: Actuation methods and mechanisms, Coordin. Chem. Rev. 320 (2016) 38-52.

[4] J. Hu, Y. Zhu, H. Huang, Recent advances in shape–memory polymers: Structure, mechanism, functionality, modeling and applications, Prog. Polym. Sci. 7 (12) (2012) 1720-1763.

[5] A. Belmonte, G. C. Lama, G. Gentile, Synthesis and characterization of liquid-crystalline networks: toward autonomous shape-memory actuation, J. Phys. Chem. C. 121 (40) (2017) 22403-22414.

[6] J. Fan, G. Li, High enthalpy storage thermoset network with giant stress and energy output in rubbery state, Nat. Commun. 2018, DOI: 10.1038/s41467-018-03094-2.

[7] J. Karger-Kocsis, S. Kéki, Review of progress in shape memory epoxies and their composites, Polymers 10 (1) (2017) 34-71.

[8] H. Xie, L. Li, X. Y. Deng, Reinforcement of shape-memory poly (ethylene-co-vinyl acetate) by carbon fibre to access robust recovery capability under resistant

condition, Compos. Sci. Technol. 157 (2018) 202-208.

[9] Z. Y. Meng, L. Chen, H. Y. Zhong, Effect of different dimensional carbon nanoparticles on the shape memory behavior of thermotropic liquid crystalline polymer, Compos. Sci. Technol. 138 (2017) 8-14.

[10] G. C. Lama, P. Cerruti, M. Lavorgna, Controlled actuation of a carbon nanotube/epoxy shape-memory liquid crystalline elastomer, J. Phys. Chem. C. 120 (42) (2016) 24417-24426.

[11] Y. Dong, H. Xia, Y. Zhu, Effect of epoxy-graft-polyoxyethylene octyl phenyl ether on preparation, mechanical properties and triple-shape memory effect of carbon nanotube/waterborne epoxy nanocomposites, Compos. Sci. Technol. 120 (2015) 17-25.

[12] R. Abishera, R. Velmurugan, K. V. N. Gopal, Reversible plasticity shape memory effect in carbon nanotubes reinforced epoxy nanocomposites, Compos. Sci. Technol. 137 (2016) 148-158.

[13] J. Lu, A. Arsalan, Y. Dong, Y. Zhu, C. Qian, R. Wang, Y. Fu, Shape memory effect and recovery stress property of carbon nanotube/waterborne epoxy nanocomposites investigated via TMA, Polym Test. 59 (2017) 462-469.

[14] R. Abishera, R. Velmurugan, K. V. N. Gopal, Reversible plasticity shape memory effect in epoxy/CNT nanocomposites-A theoretical study, Compos. Sci. Technol. 141 (2017) 145-153.

[15] R. Abishera, R. Velmurugan, K. V. Nagendra Gopal, Reversible plasticity shape memory effect in carbon nanotube/epoxy nanocomposites: Shape recovery studies for torsional and bending deformations, Polym. Eng. Sci. 58 (1) (2018) 189-198.

[16] X. Chen, M. Qiu, H. Ding, A reduced graphene oxide nanofiltration membrane

intercalated by well-dispersed carbon nanotubes for drinking water purification, Nanoscale 8 (10) (2016) 5696-5705.

[17] L. Tian, M. J. Meziani, F. Lu, Graphene oxides for homogeneous dispersion of carbon nanotubes, ACS Appl. Mater. Inter. 2 (11) (2010) 3217-3222.

[18] A. Marotta, G. C. Lama, V. Ambrogi, Shape memory behavior of liquid-crystalline elastomer/graphene oxide nanocomposites, Compos. Sci. Technol. 159 (2018) 251-258.

[19] L. Chen, W. Li, Y. Liu, Nanocomposites of epoxy-based shape memory polymer and thermally reduced graphite oxide: Mechanical, thermal and shape memory characterizations, Compos. Part B-Eng. 91 (2016) 75-82.

[20] W. Wang, D. Liu, Y. Liu, Electrical actuation properties of reduced graphene oxide paper/epoxy-based shape memory composites, Compos. Sci. Technol. 106 (2015) 20-24.

[21] W. Zhang, Z. Zhang, J. Yang, Largely enhanced thermal conductivity of poly (vinylidene fluoride)/carbon nanotube composites achieved by adding graphene oxide, Carbon 90 (2015) 242-254.

[22] Y. Dong, Q.Q. Ni, L. Li, Novel vapor-grown carbon nanofiber/epoxy shape memory nanocomposites prepared via latex technology, Mater. Lett. 132 (2014) 206-209.

[23] Z. Xu, C. Gao, Aqueous liquid crystals of graphene oxide, ACS Nano. 5 (4) (2011) 2908-2915.

[24] J. Guo, Z. Wang, L. Tong, Effects of short carbon fibres and nanoparticles on mechanical, thermal and shape memory properties of SMP hybrid nanocomposites, Compos. Part B-Eng. 90 (2016) 152-159.

[25] Y.J. Wan, L.X. Gong, L.C. Tang, Mechanical properties of epoxy composites filled with silane-functionalized graphene oxide, Compos. Part A-Appl. S. 64 (2014) 79-89.

[26] I. Zaman, H.C. Kuan, J. Dai, From carbon nanotubes and silicate layers to graphene platelets for polymer nanocomposites, Nanoscale 4 (15) (2012) 4578-4586.

[27] R. Castaldo, G. C. Lama, P. Aprea, G. Gentile, M. Lavorgna, V. Ambrogi, P. Cerruti, Effect of the oxidation degree on self-assembly, adsorption and barrier properties of nano-graphene, Micropor. Mesopor. Mat. 260 (2018) 102-115.

[28] D. Yu, K. Goh, H. Wang, Scalable synthesis of hierarchically structured carbon nanotube-graphene fibres for capacitive energy storage, Nat. Nanotechnol. 9 (7) (2014) 555-562.

[29] G. Czél, M. Jalalvand, M.R. Wisnom, Hybrid specimens eliminating stress concentrations in tensile and compressive testing of unidirectional composites, Compos. Part A-Appl. S. 91 (2016) 436-447.

[30] Y. Dong, Q.Q. Ni, Y. Fu, Preparation and characterization of waterborne epoxy shape memory composites containing silica, Compos. Part A-Appl. S. 72 (2015) 1-10.

[31] Y. Yao, Y. Luo, Y. Xu, B. Wang, Remotely actuated porous composite membrane with shape memory property, Compos. Struct. 192 (2018) 507-515.

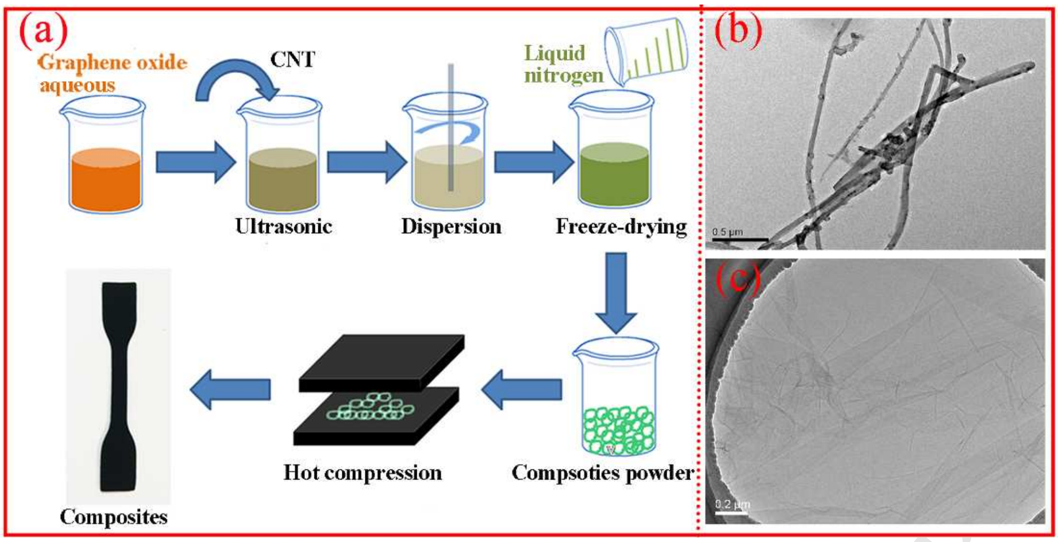

Fig. 1. (a) Preparation procedures of composites; TEM images of (b) CNT and (c) GO.

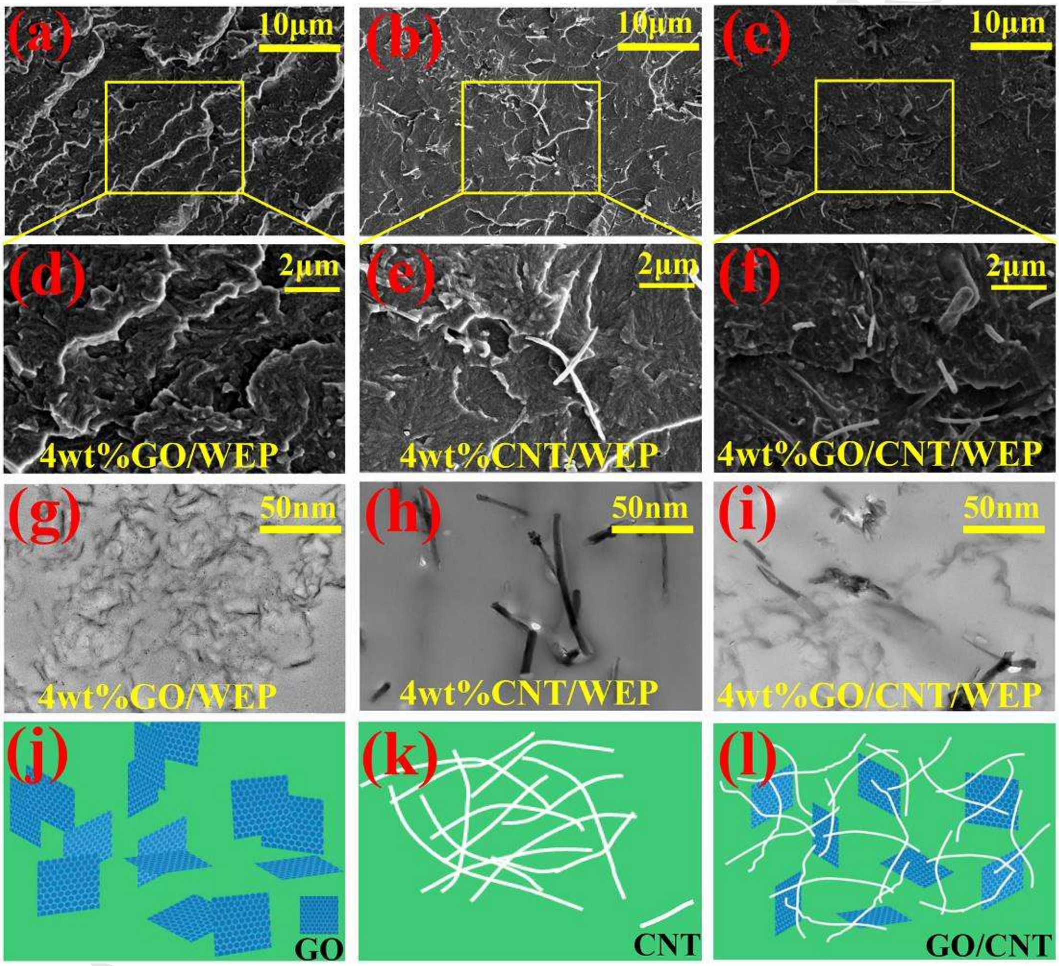

Fig. 2. SEM images of (a, d) 4wt% GO/WEP composites, (b, e) 4wt% CNT/WEP composites and (c, f) 4wt% GO/CNT/WEP composites, respectively; TEM images of (g) 4wt% GO/WEP composites, (h) 4wt% CNT/WEP composites and (i) 4wt% GO/CNT/WEP composites, respectively; Schematic of (j) 4wt% GO/WEP composites, (k) 4wt% CNT/WEP composites and (l) 4wt% GO/CNT/WEP composites, respectively.

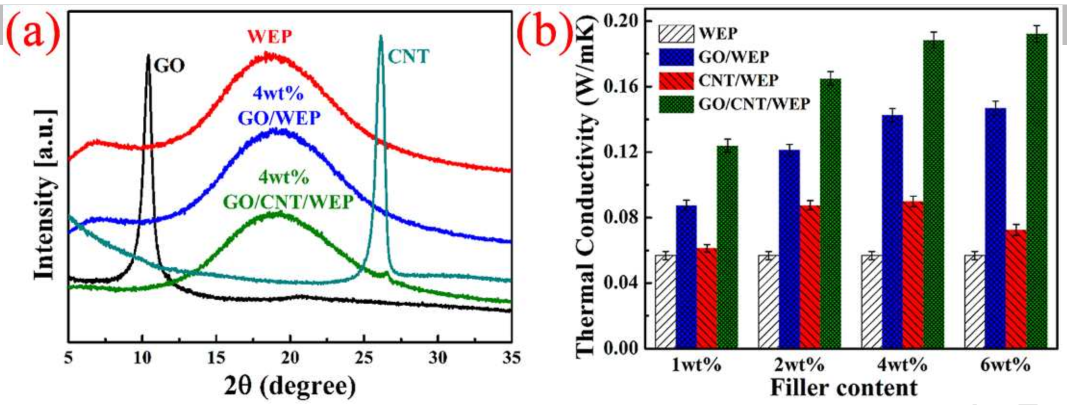

Fig. 3. (a) XRD spectra of GO, CNT, WEP, and its composites; (b) Thermal conductivity of the composites.

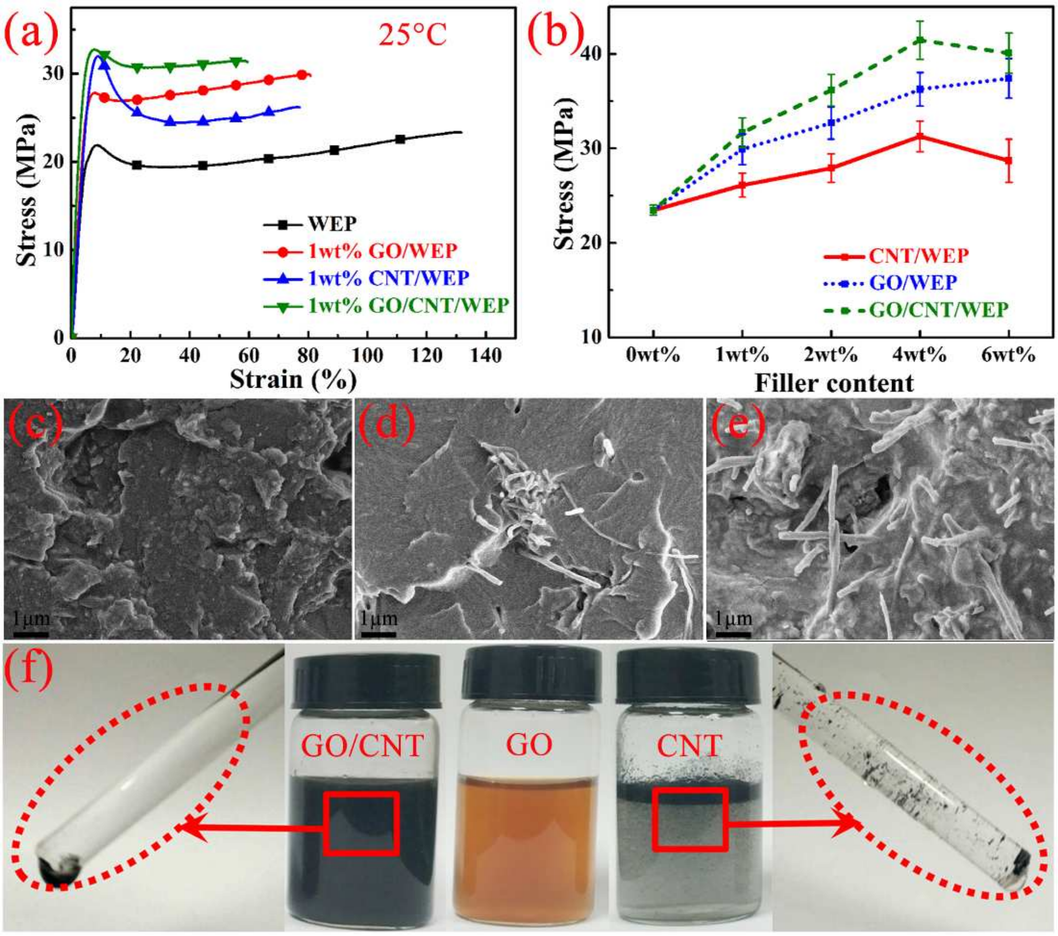

Fig. 4. (a) and (b) Mechanical properties of the composites; SEM images of (c) 6wt% GO/WEP composites, (d) 6wt% CNT/WEP composites and (e) 6wt% GO/CNT/WEP composites; (f) Photographs and dipping test show the dispersion of GO, CNT, GO/CNT in distilled water after 3 days.

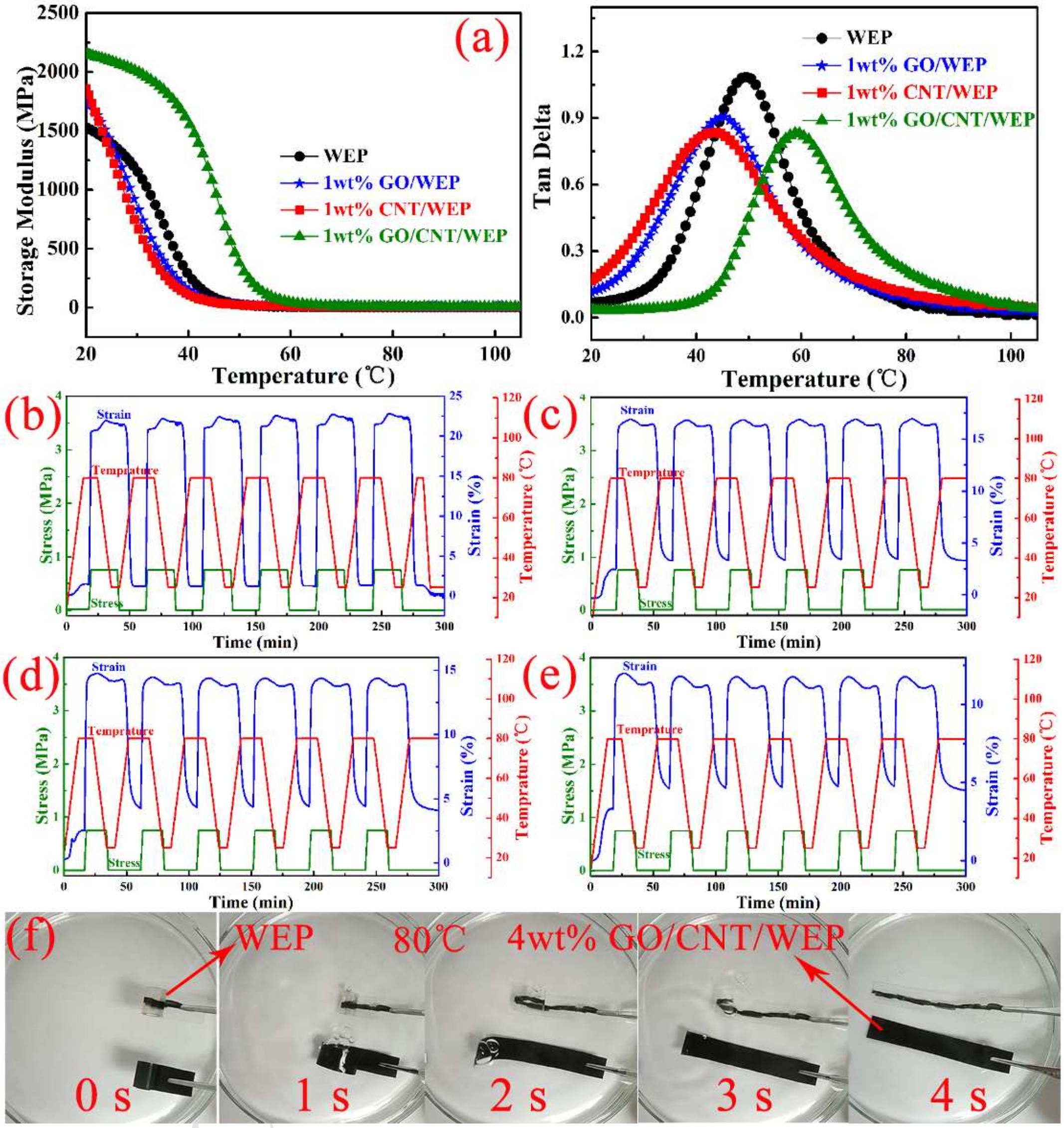

Fig. 5. (a) Storage modulus and Tan Delta of the composites; Thermal mechanical cycle of (b) WEP, (c) 4wt% GO/WEP composites, (d) 4wt% CNT/WEP composites and (e) 4wt% GO/CNT/WEP composites, respectively; (f) Shape recovery behavior of the samples at 80 °C.

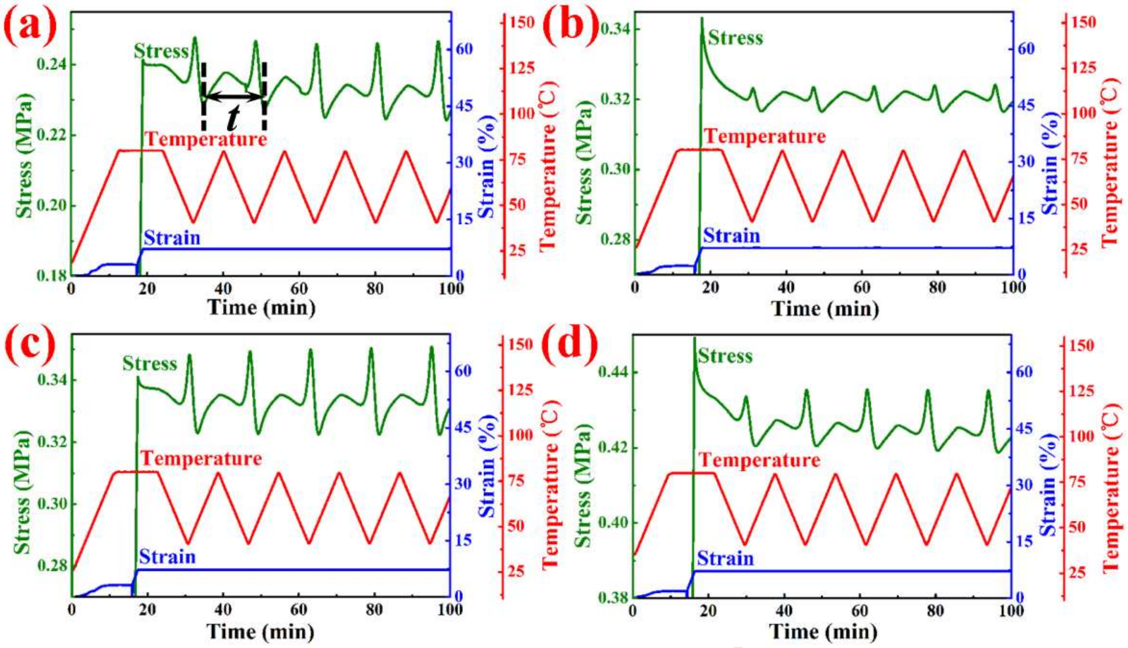

Fig. 6. Thermal response speeds of WEP and its composites: (a) WEP; (b) 1wt% CNT/WEP composites; (c) 1wt% GO/WEP composites; and (d) 1wt% GO/CNT/WEP composites.

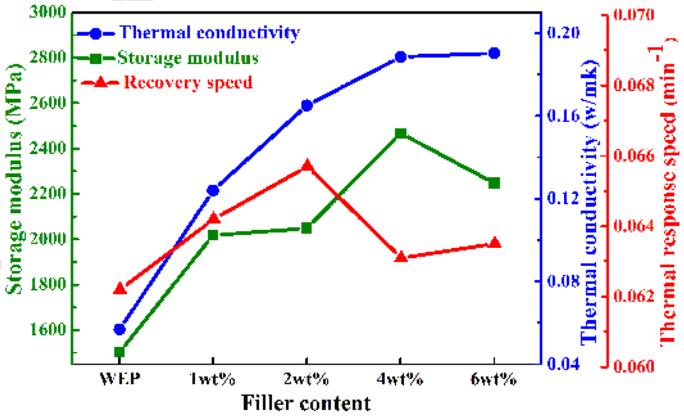

Fig. 7. Relationship of storage modulus, thermal conductivity and thermal response speeds of the GO/CNT/WEP composites.

Table 1 Properties of WEP and its composites.

Samples	Storage modulus at 20 °C (MPa)	Thermal response speed (1/*t*, min^{-1})	R_f (%)	R_r (%)	T_g (°C)
WEP	1530	0.0622	92.3	98.7	50.9
1wt%CNT/WEP	1724	0.0637	91.2	99.1	47.5
2wt% CNT/WEP	1834	0.0643	92.1	98.8	47.7
4wt% CNT/WEP	2263	0.0635	91.9	98.6	47.2
6wt% CNT/WEP	2147	0.0637	92.3	98.3	47.3
1wt% GO/WEP	1823	0.0633	93.7	98.6	48.3
2wt% GO/WEP	1952	0.0649	92.3	99.3	48.6
4wt% GO/WEP	2162	0.0633	91.8	99.2	48.3
6wt% GO/WEP	2269	0.0629	92.4	99.1	48.7
1wt%GO/CNT/WEP	2018	0.0642	91.4	99.0	60.1
2wt%GO/CNT/WEP	2049	0.0661	91.6	99.2	60.3
4wt%GO/CNT/WEP	2650	0.0631	91.5	98.3	60.6
6wt%GO/CNT/WEP	2248	0.0635	92.1	98.8	60.2